Research on Engineering Structures & Materials
www.jresm.org
Research Group

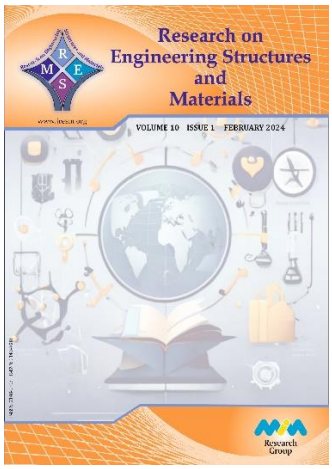


# Spectral analysis of cross-hole sonic logging data for pile integrity assessment

Ilya Lozovsky, Aleksei Churkin

Online Publication Date: 11 January 2024
URL: http://www.jresm.org/archive/resm2024.82me1115rs.html
DOI: http://dx.doi.org/10.17515/resm2024.82me1115rs
Journal Abbreviation: *Res. Eng. Struct. Mater.*

**To cite this article**
Lozovsky I, Churkin A. Spectral analysis of cross-hole sonic logging data for pile integrity assessment. *Res. Eng. Struct. Mater.*, 2024; 10(3): 1051-1063.

Research on Engineering Structures & Materials
www.jresm.org

*Research Article*

# Spectral analysis of cross-hole sonic logging data for pile integrity assessment

Ilya Lozovsky[*1,a], Aleksei Churkin[2,3,b]

[1]*Geoelectromagnetic Research Center, Branch of Schmidt Institute of Physics of the Earth, Russian Academy of Sciences, Moscow, Troitsk, Russia*
[2]*Gersevanov Research Institute of Bases and Underground Structures (NIIOSP), Research Center of Construction JSC, Moscow, Russia*
[3]*Schmidt Institute of Physics of the Earth, Russian Academy of Sciences, Moscow, Russia*

**Article Info**

*Article history:*

Received 15 Nov 2023
Accepted 11 Jan 2024

*Keywords:*

*Pile testing;*
*Nondestructive testing;*
*Ultrasonic;*
*Cross-hole sonic logging;*
*Deep foundations;*
*Bored piles*

**Abstract**

Ensuring the safety of foundations requires advanced non-destructive testing techniques. Cross-hole sonic logging (CSL) is a widely adopted method for evaluating the integrity of deep foundation elements, such as bored piles, barrettes, and diaphragm walls. This method involves analyzing the propagation time and relative energy of ultrasonic pulses transmitted and registered by probes inserted into pre-installed access tubes. However, in certain cases, standard analyses may not effectively distinguish anomalous signals arising from defects and other factors unrelated to concrete quality. Our study explores the potential of an alternative frequency-domain approach for CSL data analysis. We propose new attributes to quantify ultrasonic signal spectra, including spectrum area, normalized spectrum area, weighted mean frequency, and maximum frequency. These attributes are automatically calculated, eliminating the need for additional data processing time and minimizing the risk of human error. The proposed approach was applied to CSL data collected from two bored piles of 46 m length and successfully identified signals classified as anomalous through standard time-domain analysis. Further research is deemed necessary to fully explore the potential of the frequency-domain approach in enhancing the information content and reliability of CSL pile integrity testing.



## 1. Introduction

The safety of a building begins with a strong and reliable foundation. Bored pile foundations are esteemed for their high bearing capacity, adaptable geometry, cost-effectiveness, and minimal environmental impact. However, deviations from construction standards can introduce defects, compromising the bearing capacity and durability of these foundations. Therefore, it is imperative to employ non-destructive testing techniques capable of thoroughly assessing the structural integrity of deep foundation elements [1–3]. These techniques rely on various physical phenomena, such as ultrasound propagation [4–7], low-frequency acoustic waves [8,9], heat transfer [10,11], and others. Fig. 1 offers a comparative diagram illustrating the various non-destructive testing methods employed [3, 12-14]. These methods exhibit significant variations in their prevalence, scope, and resolution. The choice of the testing method depends on the specific issues to be addressed, structural design, soil conditions, regulatory requirements, and testing costs. The necessity for further development of non-destructive testing methods for deep foundations arises

*Corresponding author: i.n.lozovsky@gmail.com
[a] orcid.org/0000-0001-9298-6513; [b] orcid.org/0000-0002-4043-9590
DOI: http://dx.doi.org/10.17515/resm2024.82me1115rs

from the technical complexities, high costs, and limited applicability of direct quality control methods, alongside the increasing number of underground construction projects in urban settings.

Currently, cross-hole sonic logging (CSL) stands out as a widely adopted method for pile integrity testing, actively applied in practical scenarios. The testing procedure is subject to regulation by standards and technical codes in various countries [15]. However, despite its prevalence, significant variation exists in testing procedures and CSL data interpretation criteria [16]. In certain cases, current approaches to CSL data analysis may struggle to distinguish ultrasonic anomalies caused by defects and other factors unrelated to concrete quality [16]. These approaches also offer limited capabilities for evaluating the strength of concrete and identified defects [4]. Additionally, the effectiveness of current CSL data analysis techniques can be compromised by diverse sources of errors [15]. Consequently, there is a pressing need to explore novel data analysis techniques to enhance the reliability and informativeness of CSL.

In this paper, we present an approach to analyze CSL test data in the frequency domain and introduce new parameters (attributes) for quantifying recorded signal spectra. The Materials and Methods section delineates fundamental CSL testing principles, current data analysis methods, and a step-by-step procedure for attribute calculation. The Results section shares our initial experience in applying these attributes to ultrasonic signals and profiles. The Conclusions section addresses the potential and limitations of the proposed techniques.

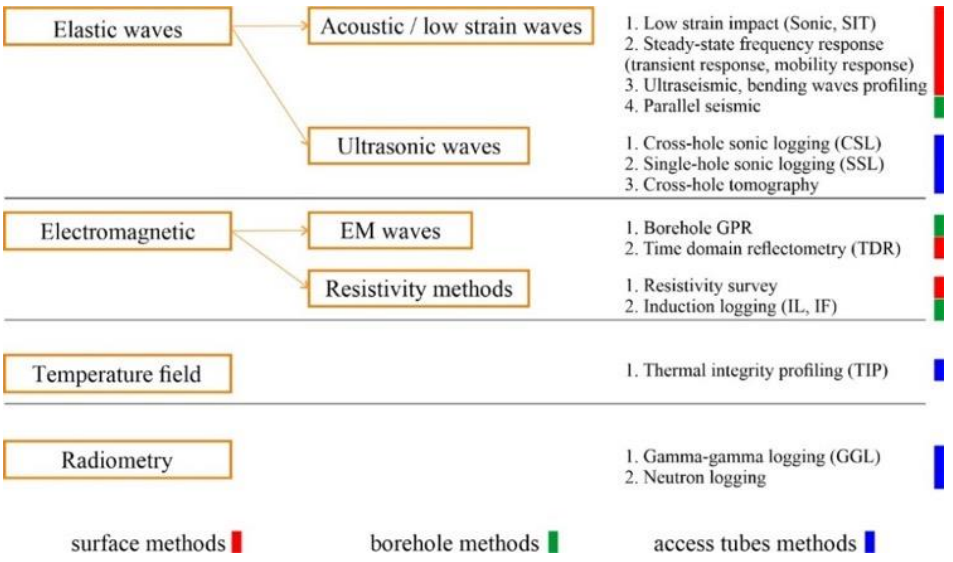


Fig. 1. Non-destructive methods for pile integrity testing. Modified from [13]

## 2. Materials and Methods

### 2.1. CSL of Deep Foundation Elements

Cross-hole sonic logging is the most common non-destructive integrity testing method for deep foundation elements with pre-installed access tubes [7]. This test relies on the analysis of ultrasonic wave propagation within the pile body. Ultrasonic waves are generated and received by ultrasonic probes, including a transmitter and at least one receiver, which are inserted into access tubes made of steel or plastic (PVC) with typical

diameters of 40 to 60 mm (Fig. 2). These access tubes are installed in the reinforcing cage during pile construction and require filling with water before testing.

The testing should be conducted no earlier than 3 to 7 days after casting. The standard testing procedure involves raising the probes synchronously from the bottom of the access tubes to the top of the structure while generating and receiving ultrasonic waves at fixed depth intervals. Subsequently, the recorded data is processed and presented graphically. The testing procedure is governed by technical codes and specifications in various countries, such as the US, UK, France, China, and others, with the ASTM D6760 code often serving as the de facto standard in many regions [7].

The method of data acquisition through access tubes determines the controlled volume of the drilled shaft body and the measurement techniques employed [4,8,17]. Cross-hole configurations are the predominant choice for the application of ultrasonic testing, whereas single-hole configurations are used less frequently [3]. Several techniques are utilized to enhance the understanding of defect properties and geometry, with cross-hole tomography representing the most advanced approach. In addition to the ray-based traveltime tomography [18], new methods are under development, including attenuation-based and full-wave inversion techniques [2,19,20].

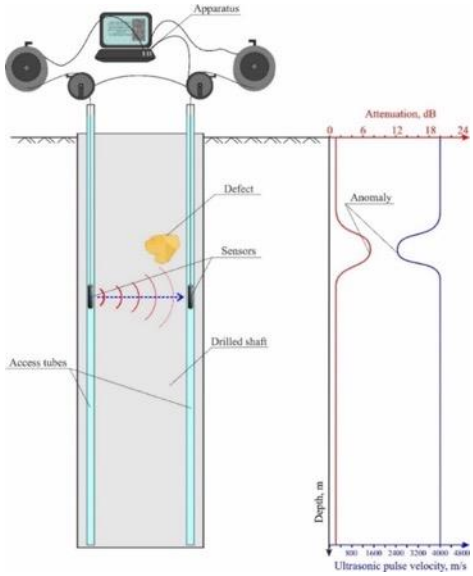


Fig. 2. CSL pile integrity testing arrangement. Modified from [4]

### 2.2. CSL Data Analysis

The results of ultrasonic measurements for each pile comprise sets of ultrasonic signals recorded in each pair of access tubes, forming ultrasonic profiles. The raw data for each ultrasonic profile is visualized as a waterfall diagram, or seismogram, where signal strength (voltage) is represented by color (Fig. 3a). Visual analysis of a waterfall diagram allows for the rapid identification of changes in signal amplitudes and first arrival times (FAT), enabling the assessment of data quality, such as signal-to-noise ratio and the choice of signal gain value.

The registered ultrasonic data is qualitatively characterized through the calculation of parameters for each recorded signal. In accordance with ASTM D6760 requirements, the set of estimated parameters should encompass the First Arrival Time (Fig. 3b) and the

Relative Energy (RE, Fig. 3c). Additionally, this list may be extended to include the Wave Speed of ultrasonic pulses.

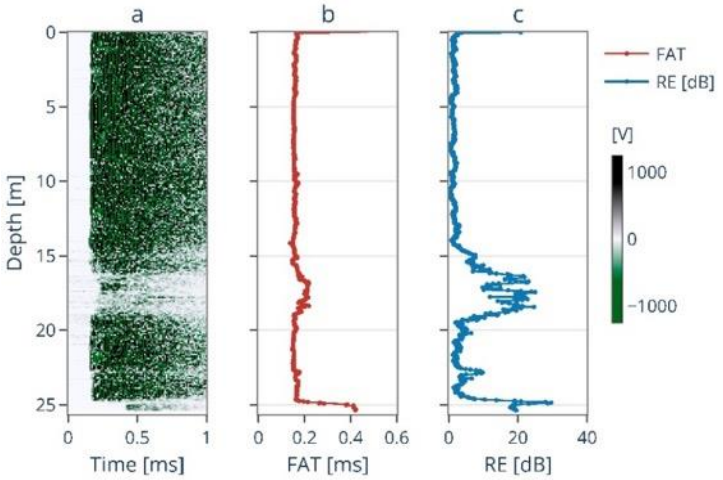


Fig. 3. An example of an ultrasonic profile for a pile with two defects: waterfall diagram (a); FAT (b) and RE (c) plots

The FAT value corresponds to the arrival time of the first waves, which travel in the fastest path between the transmitter and receiver and can be distinguished during signal analysis. To expedite the process, FAT is typically determined using automated picking algorithms [21]. However, for anomalous signals (those with low amplitude or noise), FAT estimates should be manually corrected. Following the picking procedure, the average FAT value and the deviations from the average value (%) should be calculated for each ultrasonic profile. Calculating the average FAT value should employ a robust average algorithm, as outlined in [22].

FAT values can be employed to calculate the wave speed. This calculation should consider the additional travel time in both the water and the access tube material:

$$V = L/(t_0 - 2(\frac{L_{tube}}{V_{tube}} + \frac{L_{water}}{V_{water}})) \quad (1)$$

where, $V$ – wave speed, $L$ – the distance between the probes, $t_0$ – FAT value, $L_{tube}$ – tube wall thickness, $L_{water}$ – the distance between the access tube and the ultrasonic probe in it (travel path in water), $V_{tube}$ – longitudinal wave speed in tube material (typically 5100 m/s in steel and 2300 m/s in PVC), $V_{water}$ – longitudinal wave speed in water (typically 1500 m/s).

The Relative Energy characterizes the attenuation of ultrasonic waves transmitted through the pile. According to ASTM D6760 [7], Relative Energy is defined as:

$$RE = 20\ log\frac{E}{E_0} \quad (2)$$

where, $E$ represents the energy of a given pulse, calculated by summing the absolute values of the pulse amplitudes, and $E_0$ is the reference energy, set as a constant value equal to the maximum energy of an ultrasonic profile or a fixed high value [23]. Energy values can be calculated for two preset time intervals: either for at least five cycles starting from the FAT (approximately 0.1 ms), or for the full length of the signal.

While FAT characterizes the fastest wave path between the transmitter and receiver, RE for both time intervals describe a larger area [4,23]. Therefore, it is necessary to include both FAT and RE in the analysis. In some cases, RE can be helpful in distinguishing FAT anomalies caused by defects from those unrelated to concrete quality, as discussed in [4,24].

The processed ultrasonic data should be classified into one of the categories proposed by Sellountou et al. [16]: class A (acceptable), class B (conditionally acceptable), and class C (highly abnormal), according to the rating criteria presented in Fig. 4. However, it is worth noting that the RE criteria may need slight adjustments based on the dominant frequency of ultrasonic probes. Additionally, the FAT delay values can be substituted with wave speed deviations to account for the differences in the depths of transmitter and receiver probes and the additional travel time in the water and access tube, as described in Eq. (1).

It's important to emphasize that the rating criteria presented should not be the sole means for evaluating pile quality [16]. Highly abnormal CSL data necessitate additional measurements or analysis to distinguish defects from other sources of ultrasonic anomalies and prevent misinterpretation of test results.

In CSL tests, the receiver signal represents the superposition of different types of ultrasonic waves arriving at the probe. Standard time-domain analysis is not fully able to capture and describe the complex full-wave structure of the received signals. While comprehensive full-wave analysis of CSL data is currently constrained due to inherent ambiguity of inverse problems and computational limitations, simpler yet effective techniques can be employed to complement and enhance standard time-domain procedures.

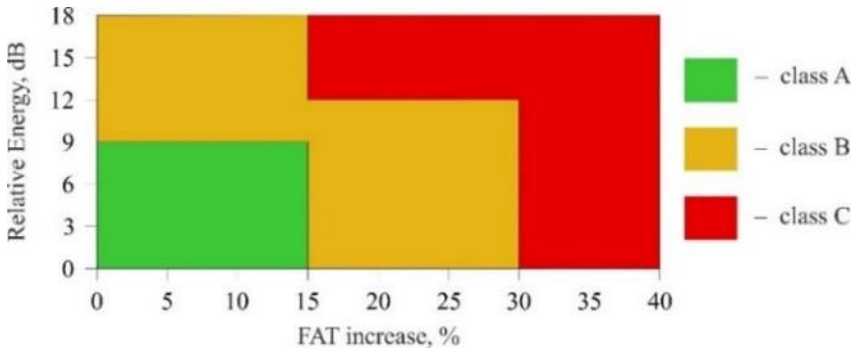


Fig. 4. Graphical representation of ultrasonic data rating criteria. Modified from [16]

### 2.3. Calculation of Spectral Attributes for CSL Data

In this section, we introduce a technique for analyzing CSL data in the frequency domain and offer a step-by-step procedure for calculating CSL data spectral attributes to complement the standard set of FAT and RE.

To begin, we convert an ultrasonic signal from the time domain to the frequency domain using the Fast Fourier Transform algorithm. This algorithm separates the input signal into components contributing at discrete frequencies:

$$A_k = \sum_{n=0}^{N-1} a_n e^{-i2\pi kn/N}, \quad k = 0, \dots, N-1, \tag{3}$$

where $\{a_k\} = a_0, \dots, a_{N-1}$ represents the input signal amplitudes, $\{A_k\} = A_0, \dots, A_{N-1}$ represents the Discrete Fourier Transform (DFT) of the input signal amplitudes, and $N$ is the number of samples.

Next, we normalize (rescale) the calculated sequence of DFT by its maximum value ($A_{max}$) to emphasize the signal's frequency content rather than its amplitudes, taking advantage of the consistent source probe signals:

$$A_k^{norm} = \frac{A_k}{A_{max}}, k = 0, \dots, N-1 \tag{4}$$

In non-destructive testing, there is a crucial requirement for regulatory control, prompting the development of formalized algorithms to analyze measurement results. To quantitatively characterize the calculated spectrum, we introduce a set of spectral attributes that have been previously proposed for the analysis of seismic microzonation data, ground-penetrating radar, slab impulse-response tests [25-26], low strain impact, and parallel seismic methods for pile integrity testing [27-28]. These attributes include spectrum area $S_n$, normalized spectrum area $S_{n\_norm}$, weighted mean frequency $f_w$, and maximum frequency $f_{max}$.

Spectrum area attributes $S_n$ and $S_{n\_norm}$ approximate the area under the spectrum graph using the trapezoidal rule:

$$S_n = \sum_{i=0}^{\frac{N}{2}} \frac{A_i + A_{i+1}}{2} df \tag{5}$$

$$S_{n\_norm} = \sum_{i=0}^{N/2} \frac{A_i^{norm} + A_{i+1}^{norm}}{2} df \tag{6}$$

Where $df$ represents the frequency resolution. The weighted mean frequency $f_w$ is calculated by the equation:

$$f_w = \frac{\sum_{i=0}^{\frac{N}{2}} f_i A_i}{\sum_{i=0}^{\frac{N}{2}} A_i} \tag{7}$$

Where $f_i$ represents spectrum frequencies. The maximum frequency $f_{max}$ is the frequency that corresponds to the maximum spectrum value.

## 3. Results

### 3.1 Spectral Attribute Analysis for Selected Ultrasonic Signals

To illustrate the proposed approach for CSL data analysis, let's examine the ultrasonic signals associated with either a defect or good quality concrete. Fig. 5 shows signals classified into class A (Fig. 5a) and class C (Fig. 5b), along with their amplitude spectra and normalized amplitude spectra. These signals were acquired using the Cross Hole Analyzer (CHAMP; Pile Dynamics, Inc., USA) instrument equipped with ultrasonic transducers featuring a nominal frequency of 45 kHz.

In the time domain, a Class C signal exhibits an increased FAT and a significant decrease in amplitudes, quantified with a FAT delay of 74% and RE of -15.1 dB (with a Class A signal used as the reference data). The spectrum of the signal associated with good-quality

concrete displays multiple peaks, with the majority of its energy concentrated between 35 – 90 kHz. In contrast, the spectrum of the signal associated with the defect exhibits a prominent peak near 45 kHz, corresponding to the dominant frequency of the ultrasonic probes. Another important distinction between the two spectra is the substantial loss of both high (>90 kHz) and low (<35 kHz) frequencies in the spectrum of the Class C signal.

The spectral attributes calculated for the analyzed signals are presented in Table 1. The Class C signal is characterized by a significantly lower value of spectrum area $S_n$, primarily due to increased signal attenuation. Additionally, the Class C signal is characterized by lower values of the normalized spectrum area $S_{n\_norm}$ and the weighted mean frequency $f_w$, resulting from a concentration of coefficients of the frequency components around the dominant frequency of the ultrasonic probes. It's noteworthy that the maximum frequency $f_{max}$ of both signals exhibits relatively close values.

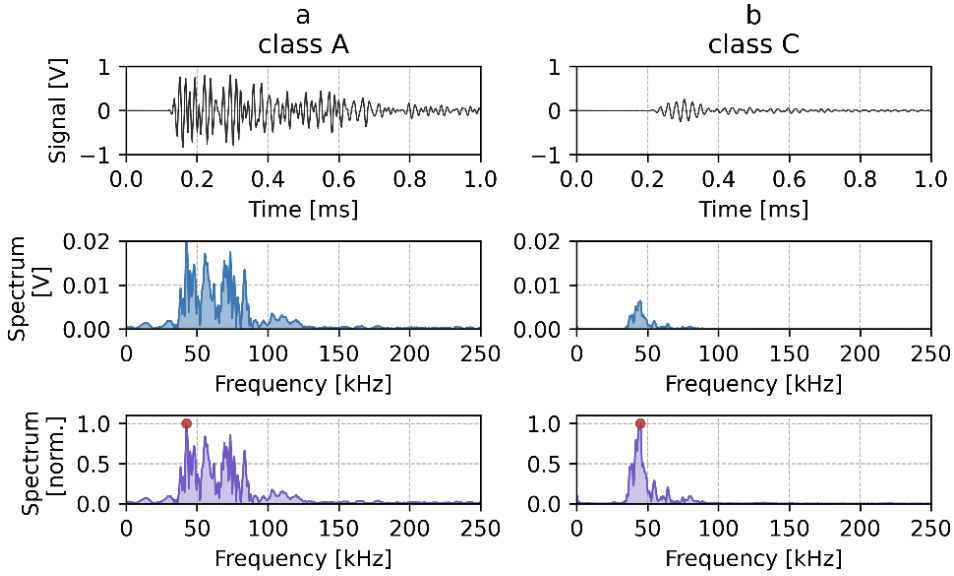


Fig. 5. Class A (a) and class C (b) ultrasonic signals, their spectra, and normalized spectra. The red dots on normalized spectra represent the maximum frequency ($f_{max}$)

Table 1. Spectral attributes of sample signals

| Signal | $S_n$ [V·Hz] | $S_{n\_norm}$ [Hz] | $f_w$ [Hz] | $f_{max}$ [Hz] |
|---|---|---|---|---|
| Class A | 565 | 27750 | 72990 | 42560 |
| Class C | 72 | 11065 | 52230 | 44950 |

### 3.2 Spectral Attribute Analysis for Ultrasonic Profiles

We proceed by examining sets of CSL data collected from two bored piles measuring 1 m in diameter and 46 m in length. The CSL data was acquired using CHAMP equipment, with measurements taken at approximately 50 mm depth intervals, following the ASTM D6760 procedure (Fig. 6). Standard time-domain analysis of the waterfall diagram, FAT and RE values for Pile 1 (Fig. 7, a-c) reveals an ultrasonic anomaly within the depth range of 41.4-41.9 m, falling somewhere between Classes B and C. A similar analysis conducted for Pile 2 (Fig. 8, a-c), has identified multiple anomalies within the depth range of 10.5 – 14.7 m, classified as Class C.

Next, we converted each ultrasonic signal into the frequency domain and displayed the ultrasonic profile data as spectrum waterfall diagrams (Fig. 7d, 8d) and normalized spectrum waterfall diagrams (Fig. 7e, 8e). Similar to standard waterfall diagrams, these representations were generated by converting each spectrum into a narrow strip where its amplitudes were color-coded, and then stacking these strips together. This approach enables us to visually compare and analyze the variations in the frequency content of ultrasonic signals with depth.

The spectra of the ultrasonic signals that were identified as anomalous in the time-domain analysis exhibit a significant reduction in amplitudes for frequencies greater than 90 kHz and less than 30 kHz. To capitalize on this observation, let's proceed with further analysis of the frequency-domain data in three distinct ranges: 0-30, 30-100, and 100-250 kHz.

For a quantitative characterization of the frequency-domain data, we have computed spectral attributes. Weighted mean frequency $f_w$ and maximum frequency $f_{max}$ calculated for these three frequency ranges are presented in subplots (f, h, j) of Figures 7 and 8. Spectrum area $S_n$ and normalized spectrum area $S_{n\_norm}$ calculated for the same frequency ranges are shown in subplots (g, i, k). Prior to plotting, the $S_n$ and $S_{n\_norm}$ graphs were normalized by their respective maximum values.

In the frequency range of 0-30 kHz, a significant reduction in the values of the proposed attributes is observed at the depth ranges identified as anomalous by the time-domain analysis. Specifically, $f_{max}$, representing the maximum spectrum amplitude in the selected frequency range, decreases by up to the first hundred Hz. $f_w$ experiences a reduction of more than 50% from its background value of 20 kHz. The significant drop in both $S_n$ and $S_{n\_norm}$ for both piles clearly indicates anomalies as well.

In the frequency range of 30-100 kHz, there is a noticeable reduction in $S_n$ for both piles, particularly influenced by the RE of the signals. However, $f_{max}$ does not provide a clear indication of anomalies. On the other hand, $f_w$ and $S_{n\_norm}$ only point to anomalies for Pile 2 (Fig. 8), associated with highly abnormal ultrasonic signals.

In the frequency range of 100-250 kHz, we observe significant local reductions in both $S_n$ and $S_{n\_norm}$, along with increases of $f_w$ values for both piles. In the case of Pile 1, $f_{max}$ does not reveal anomalies, whereas for Pile 2, it does indicate anomalies, although with a notable degree of scatter.

Fig. 6. Field photographs of the CSL testing procedure for bored piles

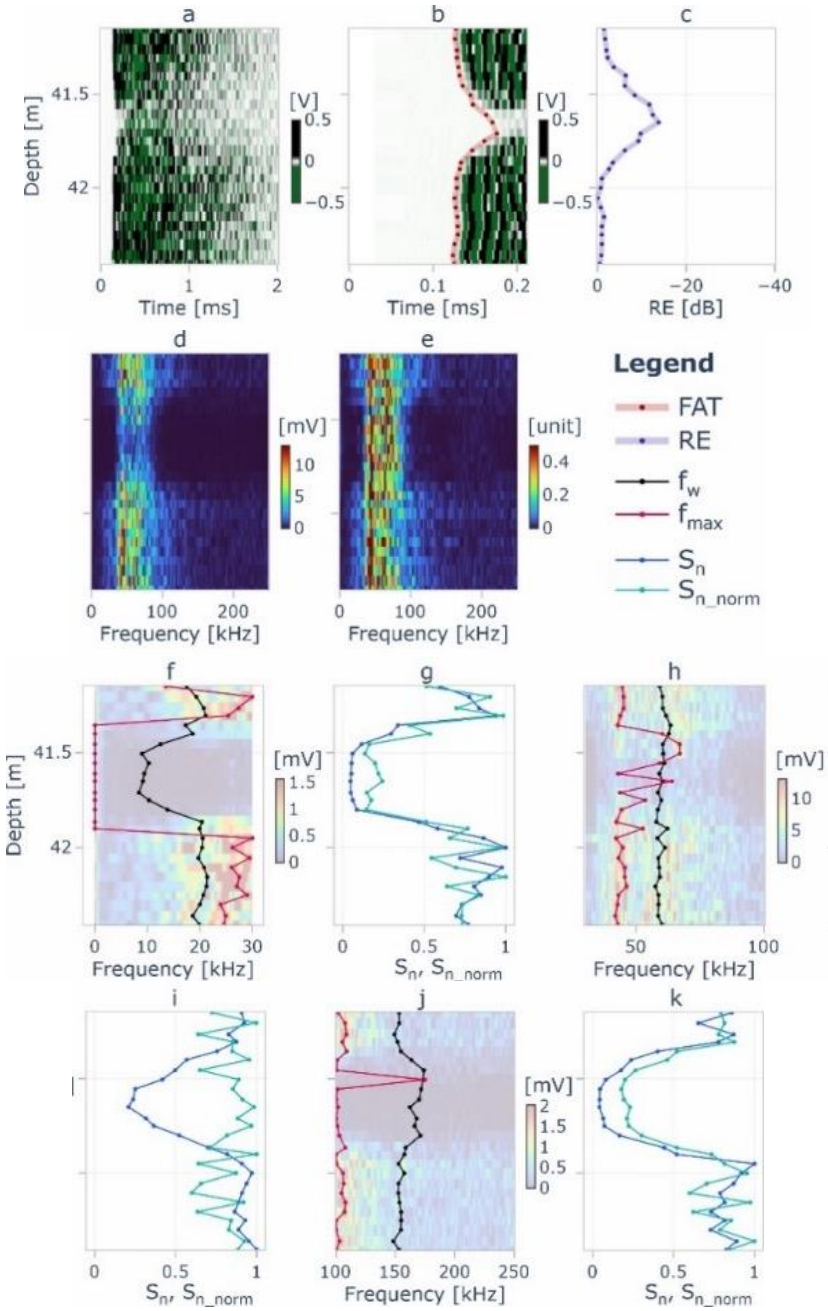


Fig. 7. CSL results from Pile 1 with an anomaly falling between Classes B and C. Subplots: (a) Waterfall diagram (full length, 2 ms), (b) FAT overlaying waterfall diagram, (c) Relative Energy, (d) Spectral waterfall diagram (full frequency range), (e) Normalized spectral waterfall diagram (full frequency range). Weighted mean frequency $f_w$ and maximum frequency $f_{max}$ (overlaid on the spectral waterfall diagram) are calculated for frequency ranges 0-30, 30-100, and 100-250 kHz and displayed in subplots (f, h, j). Spectrum area $S_n$ and normalized spectrum area $S_{n\_norm}$ calculated for the same frequency ranges are shown in subplots (g, i, k)

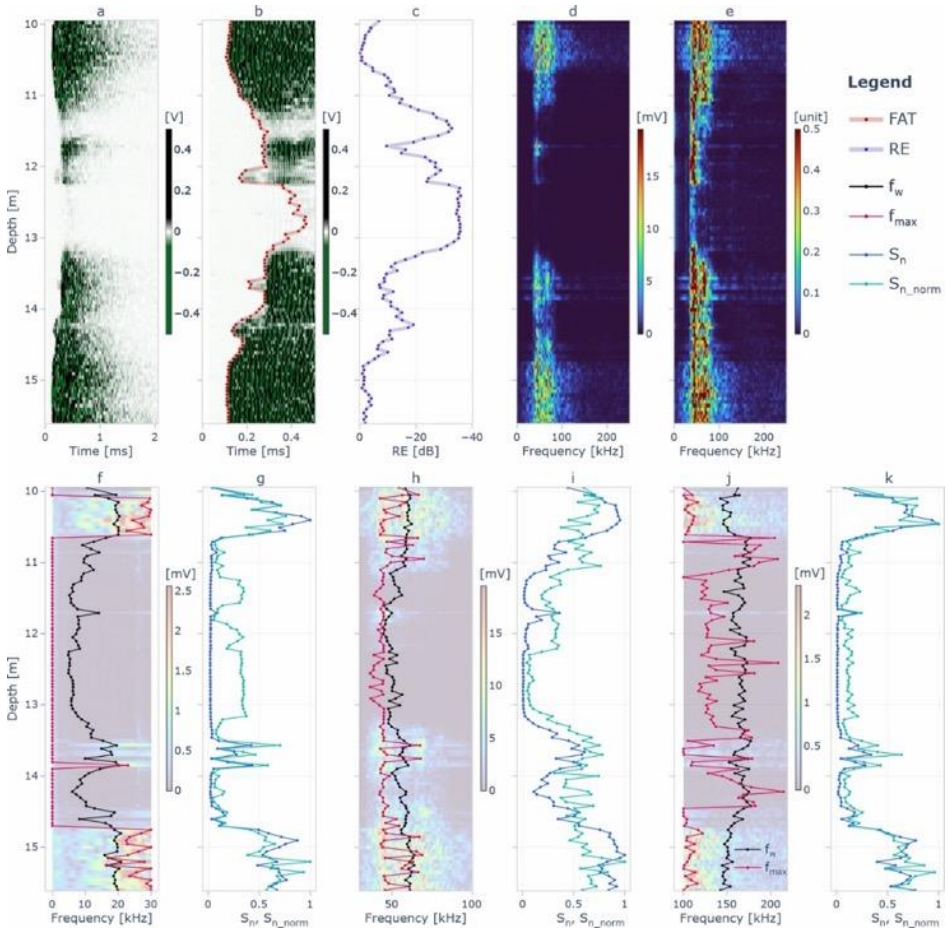


Fig. 8. CSL results from Pile 2 with several Class C anomalies. Subplot descriptions are provided in the Fig. 7 caption

## 4. Conclusions

In this study, we introduced an alternative frequency-domain approach for analyzing CSL pile integrity testing results. We proposed new attributes to quantitatively characterize frequency-domain data, including spectrum area $S_n$, normalized spectrum area $S_{n\_norm}$, weighted mean frequency $f_w$, and maximum frequency $f_{max}$. Additionally, we introduced the use of spectrum waterfall diagrams to provide a visual means of comparing and analyzing variations in the frequency content of ultrasonic signals with depth.

The proposed approach was successfully applied to examine CSL data collected from two bored piles using CHAMP equipment. The frequency-domain analysis provided results consistent with standard time-domain interpretation. Specifically, we observed a notable reduction in signal spectra amplitudes for frequencies below 30 kHz and above 90 kHz at the depth intervals recognized as anomalous in the time-domain analysis. All the spectral attributes calculated for the 0-30 kHz frequency range exhibited significant decreases at these intervals. When computed for the frequency range of 100-250 kHz, attributes $S_n$ and $S_{n\_norm}$ showed substantial reductions, while attribute $f_w$ displayed an increase at the same depth intervals.

The effectiveness of the proposed spectral attributes in identifying anomalous signals was demonstrated, offering a valuable complement to the basic set of FAT and RE. The automation of attribute calculation involves straightforward computations and eliminates the need for interactive operator involvement, thereby avoiding additional data processing time and reducing the risk of human error. Furthermore, these attributes can serve as valuable input data for tomographic inversions or signal classification using artificial neural networks.

Further research and validation efforts are essential to comprehensively assess the performance of the frequency-domain approach across diverse scenarios. This includes applying frequency-domain analysis to both numerical simulations and experimental data, involving testing piles with prefabricated defects of varying sizes, locations, and materials. Identified limitations are primarily associated with the CSL data collection process, emphasizing the need for properly selected gain and sampling rates during data acquisition. Avoiding data clipping and adhering to appropriate sampling rates, following established guidelines such as those outlined by ASTM D6760, is crucial. While there are no specific recommendations for equipment modifications, it is noted that CSL equipment used should have a broad dynamic range, a characteristic shared by most modern CSL equipment. It is important to acknowledge the potential influence of noise and artifacts on the calculated attributes, emphasizing the need for a preliminary analysis of frequency domain data, such as inspecting spectrum waterfall diagrams, to ensure the reliability of interpretation.

In summary, this study presents a promising approach to enhance CSL data analysis for detecting defects in bored piles, potentially opening the door to more advanced applications in the future.

## Acknowledgement

The research was carried out under the state task of Geoelectromagnetic Research Center, Branch of Schmidt Institute of Physics of the Earth, Russian Academy of Sciences. State task no. FMWU-2022-0023, State registration no. 122040600109-9.

## References

[1] Amir JM. Pile Integrity Testing: History, Present Situation and Future Agenda. Proceedings of the 3rd Bolivian International Conference on Deep Foundations, Santa Cruz de La Sierra, Bolivia. 2017: 17-32.

[2] Hussein MH, Goble GG. A Brief History of the Application of Stress-Wave Theory to Piles. Current Practices and Future Trends in Deep Foundations, ASCE, 2004:186-201. https://doi.org/10.1061/40743(142)11

[3] Amir JM. Pile integrity testing: All about the methods of pile NDT, 2nd edition, Piletest.com, 2020.

[4] Lozovsky IN, Zhostkov RA, Churkin AA. Numerical Simulation of Ultrasonic Pile Integrity Testing. Russ J Nondestruct Test. 2020; 56: 1-11. https://doi.org/10.1134/S1061830920010064

[5] Camp WM III, Holley DW, Canivan GJ. Crosshole Sonic Logging of South Carolina Drilled Shafts: A Five Year Summary, Contemporary Issues In Deep Foundations, ASCE, 2007.

[6] Hajali M, Abishdid C. Cross-hole sonic logging and frequency tomography analysis of drilled shaft foundations to better evaluate anomalies locations. DFI Journal. 2014; 8: 27-38. https://doi.org/10.1179/TBC14Z.0000000001

[7] D18 Committee. ASTM D6760 - 16. Test Method for Integrity Testing of Concrete Deep Foundations by Ultrasonic Crosshole Testing, 2016.
[8] White B, Nagy M, Allin R. Comparing cross-hole sonic logging and low-strain integrity testing results. The Application of Stress-Wave Theory to Piles: Science, Technology and Practice, Lisbon, Portugal. 2018: 471-476.
[9] D18 Committee. ASTM D5882 - 16. Test Method for Low Strain Impact Integrity Testing of Deep Foundations, 2016.
[10] D18 Committee. ASTM D7949 - 14. Test Methods for Thermal Integrity Profiling of Concrete Deep Foundations, 2014.
[11] Johnson KR. Analyzing thermal integrity profiling data for drilled shaft evaluation. DFI Journal 2016; 10: 25-33. https://doi.org/10.1080/19375247.2016.1169361
[12] Coe JT, Mahvelati S, Asabere P. Application of non-destructive testing and geophysical methods to evaluate unknown foundation geometry. Proceedings of 29th Central Pennsylvania Geotechnical Conference, Hershey, Pennsylvania, USA, 2017.
[13] Churkin A. Development of geophysical complex application technique for buried monolithic structures quality control, Ph.D. Thesis, Moscow State University, Moscow, 2020.
[14] Gao T. A Critical Analysis of Existing Intelligent Analytical Techniques for Pile Integrity Test. Proceedings of the 8th International Conference on Hydraulic and Civil Engineering: Deep Space Intelligent Development and Utilization Forum (ICHCE), Xi'an, China, 740-751, 2022. https://doi.org/10.1109/ICHCE57331.2022.10042772
[15] Amir JM, Amir EI. Critical Comparison of Ultrasonic Pile Testing Standards. The Application of Stress-Wave Theory to Piles: Science, Technology and Practice, Lisbon, Portugal, 2008.
[16] Sellountou AE, Amir JM, Chernauskas L, Hertlein B, Kandaris P, Kovacs T, et al. Terminology and evaluation criteria of crosshole sonic logging (CSL) as applied to deep foundations. DFI, 2019. http://www.dfi.org/viewpub.asp?tid=WP-CSL-2019 (accessed October 8, 2023).
[17] Amir JM, Amir EI. Capabilities and Limitations of Cross Hole Ultrasonic Testing of Piles. Contemporary Topics in Deep Foundations, Orlando, USA, 536-543, 2009. https://doi.org/10.1061/41021(335)67
[18] Lozovsky IN, Churkin AA, Zhostkov RA. Localization of Defects in Bored Pile Physical Model Using Cross-Hole Ultrasonic Tomography. Bull Russ Acad Sci Phys 2020; 84: 215-9. https://doi.org/10.3103/S1062873820020203
[19] Kordjazi A, Coe JT. An Experimental Design Approach for Structural Integrity Testing of Drilled Shafts Using Full Waveform Inversion. IFCEE 2021, Dallas, USA, 453-462, 2021. https://doi.org/10.1061/9780784483404.041
[20] Kordjazi A, Coe JT, Afanasiev M. Nondestructive Evaluation of Drilled Shaft Construction Anomalies Using Full Waveform Tomography of Simulated Crosshole Measurements. J Nondestruct Eval 2020; 40: 3. https://doi.org/10.1007/s10921-020-00728-8
[21] Amir EI. Determining First Arrival Time and Wave Speed in Cross-Hole Ultrasonic (CSL). Piletest.com, 2016. https://www.piletest.com/show.asp?id=Engineer (Access Date: October 1, 2023).
[22] JGJ 106-2014. Technical code for testing of building foundation piles, 2014.
[23] Amir EI. Relative Energy in Cross-Hole Ultrasonic (CSL). Piletest.com, 2016. https://www.piletest.com/show.asp?id=Engineer (Access Date: 1, 2023).
[24] Amir JM, Amir EI, Felice CW. Acceptance criteria for bored piles by ultrasonic testing. Proceedings of the 7th International Conference on the Application of Stress wave Theory to Piles, Kuala Lumpur, Malaysia, 2004.
[25] Churkin AA, Khmel'nitskii AY, Kapustin VV. Evaluation of soil-structure contact state by normalized acoustic response analysis. Soil Mech Found Eng 2022; 59: 453-458. https://doi.org/10.1007/s11204-022-09836-1

[26] Lozovsky IN, Churkin AA. Multiscale entropy analysis for slab impulse response testing. Bull Russ Acad Sci Phys. 2023; 87(10): 1518-1522. https://doi.org/10.3103/S1062873823703604

[27] Kapustin VV, Churkin AA. Assessment of the Contact between Piles and Soil via the Dynamic Attributes of Acoustic Signals. Moscow Univ Geol Bull. 2020; 75: 435-45. https://doi.org/10.3103/S0145875220040092

[28] Shmurak DV, Churkin AA, Lozovsky IN, Zhostkov RA. Spectral Analysis of Parallel Seismic Method Data for Surveying Underground Structures. Bull Russ Acad Sci Phys. 2022; 86: 79-82. https://doi.org/10.3103/S1062873822010221